OPTICAL DETERMINATION OF MECHANICAL AND STRENGTH PROPERTIES OF EPOXY BIDIRECTIONAL COMPOSITE MATERIALS REINFORCED WITH GLASS AND CARBON USING DIGITAL IMAGE CORRELATION

Krzysztof CIECIELĄG*

*Faculty of Mechanical Engineering, Department of Production Engineering,
Lublin University of Technology, Nadbystrzycka 36, 20-618 Lublin, Poland

k.ciecielag@pollub.pl

received 29 May 2026, revised 23 July 2026, accepted 24 July 2026

Abstract: This study presents a comprehensive experimental characterization of autoclave-cured bidirectional GFRP and CFRP laminates. Since prepreg manufacturers typically provide only limited information on the properties of the final cured laminates, experimental characterization is necessary to obtain the engineering constants required for finite element modeling. The experimental program enables a consistent comparison of the mechanical and strength properties of both composite systems under identical manufacturing and testing conditions. Due to the anisotropic nature of composites, the mechanical properties were determined in the principal material directions corresponding to the fiber orientation. Material specimens were prepared for testing in accordance with standards for tensile (ASTM D3039), compressive (ASTM D6641), and shear (ASTM D3518) testing. The specimens were made from prepregs, which were then cured in an autoclave. Mechanical tests were conducted using the non-contact Digital Image Correlation (DIC) technique on a testing machine. Using this optical technique, displacements and strains in composite specimens can be measured. Based on the recorded strain fields, stress-strain characteristics were determined and used to define the material parameters. Tests of mechanical and strength properties allowed for the determination of Young's modulus, shear modulus, Poisson's ratio, as well as tensile, compressive, and shear strengths. The obtained results form the basis for further numerical analyses and the validation of computational models.

Key words: polymer composites, optical determination, mechanical properties, strength properties

1. INTRODUCTION

Numerical simulations are a useful tool for reproducing the behavior of real-world systems using mathematical models and computer algorithms. The main aim of developing this field is to analyze phenomena that are costly, time-consuming, and difficult to study under real-world conditions [1]. They also allow, at the design stage, for predicting process paths, analyzing various solutions, and optimizing them without the need to conduct experiments [2]. Advancing computer technology enables the performance of highly complex calculations in a reasonable amount of time [3]. The reliability of numerical calculations performed by computer programs depends directly on the quality of the input data, such as experimentally determined material parameters. For commercially available prepregs, manufacturers usually provide only general material information, whereas the complete mechanical and strength properties of the final autoclave-cured laminate required for finite element modeling are not available. Therefore, comprehensive experimental characterization of the manufactured composite is necessary before reliable numerical analyses can be performed. The mathematical model and program algorithms, based on material data, define and predict how the simulation process will be carried out. Before performing numerical simulations, it is necessary to conduct laboratory tests to determine mechanical properties such as Young's modulus, shear modulus, and Poisson's ratio, as well as tensile, compressive, and shear strength. Experimental studies are particularly important for determining the material properties of polymer composites [4]. These are heterogeneous, anisotropic materials manufactured using several known production techniques [5]. Their mechanical and strength properties depend primarily on the fiber and matrix types and the manufacturing parameters [6]. Determining the parameters in polymer composites requires more complex testing than for homogeneous materials. The main methods used to study deformations and determine strength parameters, particularly in polymer composites, include strain gauging and optical techniques, each with its own advantages and disadvantages [7]. The basis of the first of these methods is strain gauge strain measurement, which guarantees very high measurement accuracy, but the measurement itself is only point-based [8]. Another disadvantage is the need for contact with the specimen, and in the case of heterogeneous materials such as polymer composites, their application is more debatable. The arrangement of fibers and matrix in a polymer composite is responsible for local changes in the material's properties and strength. In scientific research, strain-gauge-based techniques are widely used in unidirectional polymer composites [9]. This technology was employed to determine the mechanical properties of the entire composite and its individual components. Using tensile and shear tests on the composite, it was possible to determine isotropic material parameters [9]. By utilizing the phenomenon of electrical resistance and its measurement in carbon fiber reinforced plastics, it is possible to measure deformations under tensile stress [10]. It has also been demonstrated that changes in the electrical properties of polymer composites correlate with deformation and material damage [11]. The testing methodology using strain gauges shows that, for this purpose, it is also necessary to properly prepare the specimens in accordance with the standards [8]. The use of strain gauging allows for the very precise, point-by-point determination of the properties of carbon fiber reinforced plastics and the determination of Young's modulus, transverse elastic modulus, Poisson's ratio, ultimate stress, and strain [12]. The tests also allow determination of the properties of transversely isotropic carbon fiber composite materials, which were compared with results from ultrasonic tests [13]. Strain gauging can also be used to determine data for longitudinal and transverse tensile testing and for longitudinal compression testing of cross-woven carbon fiber composites [14].

Investigations of the properties of polymer composites often require more complex techniques [15]. This group includes Digital Image Correlation (DIC), which involves analyzing images of the specimen surface to observe deformation under load [16,17]. The advantage of this method is non-contact measurement and the ability to obtain a full strain field [18,19]. These are particularly desirable features when determining the properties of heterogeneous polymer composites [15]. The disadvantages of this method include more complex data analysis and the need for high-quality and expensive optical equipment [20]. The Digital Image Correlation technique is successfully used to determine the parameters of composites [21]. The effectiveness of Digital Image Correlation in the analysis of composites is demonstrated by numerous scientific studies, the number of which is steadily growing [22]. Digital Image Correlation is used to characterize the mechanical properties of various hybrid composite types in tensile tests. This method allows the determination of Young's modulus and tensile strength and, thanks to measurements in both the longitudinal and transverse directions, also enables the determination of Poisson's ratio [23]. DIC also allows tracking the development of strain fields in composites with various fiber types. This enables the detection of strain distributions resulting from loading that differ from the normal distribution throughout the composite material [24]. DIC technology also enables the determination of the Young's modulus of carbon fiber reinforced plastics (CFRP) subjected to aging under the influence of time and temperature [16]. This technology is also used in tensile and adhesion testing of composite reinforcements. Using DIC enables determination of a crack's location and width, as well as the mechanism of load transfer through the composite fibers [25]. By leveraging DIC's real-time visualization of the tested objects, this technique can also be combined with FEM analysis to monitor crack propagation in steel-composite joints [26]. The Digital Image Correlation technique also performs very well in fatigue tests, allowing for the observation of delamination in CFRP [27]. Delamination in polymer composites is a very common phenomenon, which is why it is frequently the subject of research. The combination of DIC with FEM enables a more complex analysis of this effect [28]. Numerical models can be experimentally validated using the 3D Digital Image Correlation technique [29]. Thanks to the composite material failure model developed based on the Hashin criterion and validated using DIC, it is possible to predict crack initiation and propagation without costly laboratory testing [29]. The analysis of composite damage images obtained from DIC has also been extended to include neural networks. Thanks to this approach, it is possible to classify DIC strain field images at the pixel level [30]. Digital Image Correlation is used not only for laboratory testing but also for finished engineering products. One example of the effective use of DIC for analyzing composite structures is its application to the inspection of helicopter rotor blades [31]. The combination of three-dimensional DIC with photogrammetry also allows for the detection of cracks in the helicopter fuselage, which is made of glass fiber reinforced plastics (GFRP) [32].

Despite the extensive application of Digital Image Correlation for the characterization of composite materials, the available literature provides only limited information on complete experimental datasets describing the mechanical and strength properties of autoclave-manufactured bidirectional GFRP and CFRP laminates produced from commercial prepregs under identical manufacturing and testing conditions. Such comprehensive datasets are essential for reliable finite element modeling and experimental validation of numerical analyses.

Therefore, the aim of this study is to experimentally determine a complete set of engineering constants and strength parameters for autoclave-cured bidirectional GFRP and CFRP laminates using standardized ASTM procedures and Digital Image Correlation. Furthermore, the study aims to provide a consistent comparison of both composite systems manufactured under identical conditions and to establish a reliable experimental database for future finite element simulations of polymer composite structures and machining processes.

2. RESEARCH METHODOLOGY

2.1. Material specimens

Material specimens for testing the mechanical and strength properties of polymer composites based on glass and carbon fibers impregnated with epoxy resin were prepared in accordance with ASTM standards. These specimens were made from prepreg fabrics with a thickness of 0.25 mm. The standards precisely specify the dimensions and method of specimen preparation, as well as the conditions for conducting measurements. Material specimens for tensile testing were prepared in accordance with ASTM D3039 [33], which recommends specimens with dimensions of 250 x 25 x 2.5 mm (length x width x thickness). The ASTM D3039 standard also specifies the manufacturing tolerances for the specimens. It allows a tolerance of +/-1% on the width dimension, corresponding to +/-0.25 mm, and a tolerance of +/-4% on the thickness dimension, corresponding to +/-0.1 mm. The compression test was performed on material specimens prepared in accordance with ASTM D6641 standard [34]. In accordance with this standard, specimens measuring 155 x 25 x 3.33 mm were prepared, with a tolerance of +/-1% (+/-0.25 mm) for width and +/-2% (+/-0.067 mm) for thickness. Material specimens for shear testing were prepared in accordance with ASTM D3518 standard [35]. The specimen dimensions recommended by the standard for shear testing at a +/-45° angle are 250 x 25 x 3 mm. The tolerances for width and thickness are +/-1 % and +/-4 %, respectively, which translate to linear dimensions of +/-0.25 mm (for width) and +/-0.12 mm (for thickness). The length and width of material specimens for shear testing are identical to those for tensile testing, with the exception that 8, 12, or 16 layers are recommended for fabrics. In the present study, 12-layer specimens were prepared for shear testing, corresponding to a thickness of 3 mm. Seven specimens of each type were prepared for two different composite materials. Each specimen was fitted with tabs at the ends to allow for mounting in a testing machine. Fig. 1 shows the detailed dimensions of the material specimens.

Glass fiber reinforced plastic (GFRP) specimens impregnated with epoxy resin were fabricated from prepregs in the form of HexPly 916G/7781/50±2.5% fabrics. In turn, material specimens of a carbon fiber reinforced plastic (CFRP) composite impregnated with epoxy resin were made from prepregs in the form of HexPly 6376/40%/285-H5/T300-3K/1200 fabric. Both prepregs are manufactured by Hexcel. The prepreg designation includes a description of the fibers and resin in its composition.

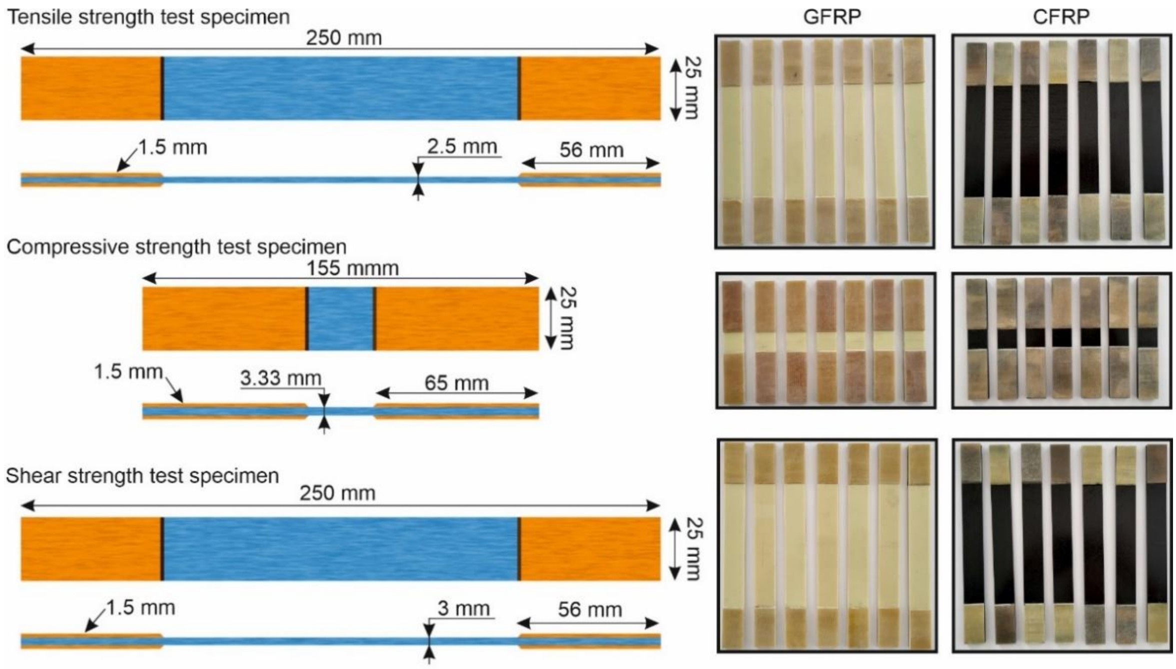

Fig. 1. Dimension scheme for material specimens used to determine mechanical and strength properties

In the name of the HexPly 916G/7781/50+/-2.5% prepreg, 916G specifies the type of thermosetting epoxy resin, which has a density of 1.30 g/cm^3. In the name 7781, it specifies the type of fabric arranged in an 8H satin weave made of glass fibers (type E) with a weight of 299 g/m^2. The final part of the description of a single layer of prepreg with a thickness of 0.25 mm specifies the resin weight content (50% ±2.5%). The designation HexPly 6376/40%/285-H5/T300-3K/1200 includes the type of thermosetting polymeric epoxy resin 6376 with a density of 1.31 g/cm^3. Furthermore, the name includes the weight percentage of resin in the prepreg, which is 40%, and the average fabric weight of 285 g/m^2 with a 5H satin weave (285-H5). The last part of the name describes the type of carbon fiber fabric (T300-3K), with a T300 class and a fiber count of 3,000 (3K). The number 1200 specifies the roll width in mm on which the prepreg is wound, with a thickness of 0.25 mm.

The composite specimens were manufactured using an autoclave process, with critical parameters including temperature, pressure, and curing time. The temperature and pressure responsible for polymerization were 175°C and 0.4 MPa, and the curing time was 2.5 hours.

2.2. Investigations of mechanical and strength properties

After the material specimens were prepared, they were tested to determine their mechanical and strength properties. Before testing, the specimens were measured and painted white and black to ensure the tested objects were visible to the cameras. The tests were conducted on an MTS 250 testing machine using the ARAMIS SRX system, which employs Digital Image Correlation (DIC) technology. The ARAMIS SRX is equipped with 12 MPx cameras, 8 GB of internal memory, and a 10G network interface. The use of Digital Image Correlation (DIC) technology enabled the measurement of displacement and strain fields, as well as the behavior of composite specimens during tensile, compressive, and shear testing. Prior to conducting the tests, the measurement system was calibrated according to the observed field of view, which was 155 x 130 x 50 mm. Calibration involved setting the distances and angles between the cameras and the test specimens. A scheme of the test setup for determining the mechanical and strength properties of polymer composites is shown in Figure 2.

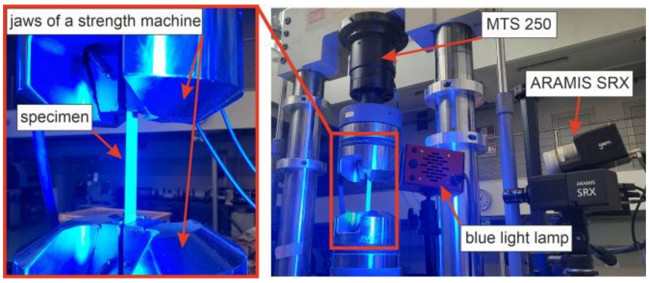

Fig. 2. Schematic of the test stand for measuring mechanical and strength properties

The research station was equipped with test heads in which the material specimens were mounted. For the compression tests in accordance with ASTM D6641, a special THS705-4G-W40-BP fixture was used, which applies a frontal load, enabling precise determination of the material's compressive strength. The compression testing device is mounted between the jaws of the testing machine. The tests were conducted at a temperature of 24°C. Conducting the tests also involves using appropriate crosshead speeds for the testing machine's jaws. For tensile, compressive, and shear tests in accordance with ASTM standards, crosshead speeds of 2 mm/min, 1.3 mm/min, and 2 mm/min were used, respectively. Thanks to the tests conducted, it was possible to determine mechanical properties such as Young's modulus, Poisson's ratio, shear modulus, and tensile, compressive, and shear strengths.

In the first stage of the research, tensile tests were conducted on specimens made of polymer composites with glass and carbon fibers, in accordance with ASTM D3039, to determine the Young's modulus E_{12}, Poisson's ratio v_{12}, the tensile force F_t, and the tensile strength σ_t. Young's modulus E_{12}, which is identical in both directions for the fabrics, was determined based on equation (1):

$$E_{12} = \frac{\Delta\sigma}{\Delta\varepsilon_l} = \frac{\sigma'' - \sigma'}{\varepsilon_l'' - \varepsilon_l'} \quad (1)$$

where
σ' – tensile stress at longitudinal strain ε_l',
σ'' – tensile stress at longitudinal strain ε_l'',
ε_l' – longitudinal strain equal to 0.05%,
ε_l'' – longitudinal strain equal to 0.25%.

In equation (1), the tensile stresses σ' and σ'' are calculated using equation (2):

$$\sigma = \frac{F_t}{A_t} \quad (2)$$

where
F_t – tensile force for longitudinal strain at ε_l' = 0.05% and ε_l'' = 0.25%,
A_t – cross-sectional area of the specimen measured prior to tensile testing [mm^2].

The Poisson's ratio is the ratio of transverse strain to longitudinal strain, calculated using the following equation (3):

$$\nu_{12} = \frac{\Delta\varepsilon_t}{\Delta\varepsilon_l} = \frac{1}{2}\left(\frac{\varepsilon_t'}{\varepsilon_l'} + \frac{\varepsilon_t''}{\varepsilon_l''}\right) \quad (3)$$

where
ε_t' – value of transverse strain corresponding to longitudinal strain 0.05%,
ε_t'' – value of transverse strain corresponding to longitudinal strain 0.25%.

The tensile strength σ_t is calculated using the following formula (4):

$$\sigma_t = \frac{F_{tmax}}{A_t} \quad (4)$$

where: F_{tmax} – maximum tensile force before specimen failure [N].

Compression tests were then conducted in accordance with ASTM D6641, during which the compressive strength σ_c was determined using Equation (5):

$$\sigma_c = \frac{F_{cmax}}{A_c} \quad (5)$$

where
F_{cmax} – maximum compressive force before specimen failure [N],
A_c – cross-sectional area of the specimen measured prior to the compression test [mm^2].

The final stage of the testing involved shear tests, conducted in accordance with ASTM D3518, during which the shear modulus G_{12} and the shear strength τ_s were determined. Similar to Young's modulus, the shear modulus is identical for both fiber orientations and is calculated using Equation (6):

$$G_{12} = \frac{\Delta\tau}{\Delta\gamma} = \frac{\tau_{12}'' - \tau_{12}'}{\gamma_{12}'' - \gamma_{12}'} \quad (6)$$

where
τ_{12}' – shear stress value at shear strain γ_{12}',
τ_{12}'' – shear stress value at shear strain γ_{12}'',
γ_{12}' – shear strain equal to 0.1%,
γ_{12}'' – shear strain equal to 0.5%.

In equation (6), the shear stress τ_{12}' and τ_{12}'' are calculated using equation (7):

$$\tau_{12} = \frac{F_S}{2 \cdot A_S} \quad (7)$$

where
F_s – shear force for a shear strain γ_{12}' = 0.1% and γ_{12}'' = 0.5%,
A_s – cross-sectional area of the specimen measured prior to the shear test [mm^2].

The final parameter determined during the shear tests was the shear strength τ_s, calculated using equation (8):

$$\tau_s = \frac{F_{smax}}{2 \cdot A_S} \quad (8)$$

where: F_{smax} – maximum shear force before specimen failure [N].

The tests were conducted until the material specimens were destroyed, in accordance with ASTM D3039, ASTM D6641, and ASTM D3518.

3. RESULTS, ANALYSIS AND DISCUSSION

Tensile, compressive, and shear tests conducted on polymer composites made it possible to determine the force-time curves, obtained directly from the testing machine. Based on the force-time curves, it is possible to determine the maximum force for each specimen type and material at which the specimen was destroyed. The obtained force values and the strain values determined using the ARAMIS SRX system enabled the determination of the mechanical and strength parameters of each tested composite material. Force-time curves for the tensile testing of glass fiber reinforced plastics (GFRP T1, GFRP T2, GFRP T3, GFRP T4, GFRP T5, GFRP T6, GFRP T7) and carbon fiber reinforced plastics (CFRP T1, CFRP T2, CFRP T3, CFRP T4, CFRP T5, CFRP T6, CFRP T7) are shown in Fig. 3.

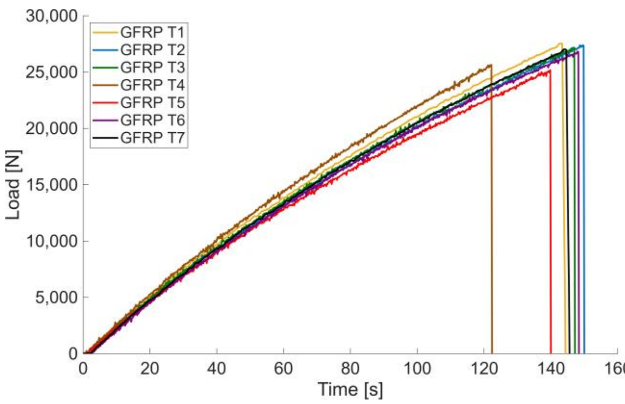

a)

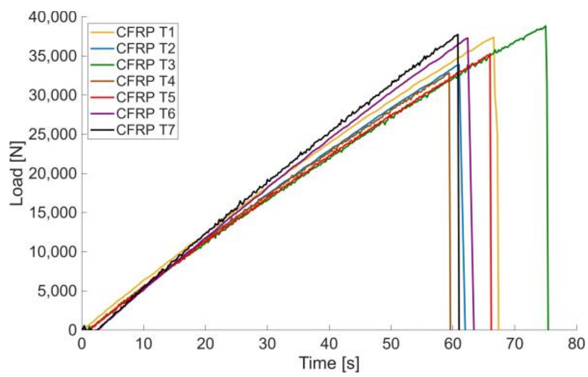

b)

Fig. 3. Force-time curves during tensile testing of GFRP (a) and CFRP (b)

DOI: 10.65731/ama/2026-0068

Based on the force-time curves, it is possible to determine the average maximum tensile force during the tensile test. The average maximum tensile breaking force for GFRP was 26,568.75 N, and for CFRP, this value was 36,109.25 N. Taking into account the average cross-sectional area of the specimens, which was 62.58 mm² (GFRP) and 62.55 mm² (CFRP), the tensile strength is 425.1 MPa for GFRP and 577.4 MPa for CFRP. The use of Digital Image Correlation (DIC) enabled visualization of the effect immediately before and after the specimen fracture, as shown in Fig. 4. A local accumulation of strain is evident, and the percentage strain relative to the original length is indicated by the scale.

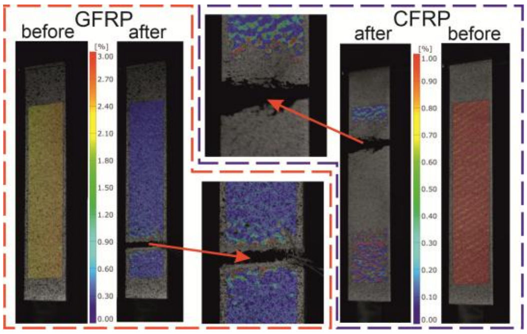

Fig. 4. Visualization of tensile test specimens made of GFRP and CFRP

The next stage of the research involved conducting compression tests on polymer composites in accordance with ASTM D6641. The specimens, mounted in the THS705-4G-W40-BP fixture within the testing machine's jaws, enabled stable compression testing of the composite specimens. Figure 5 shows the force-time curves for compressed specimens made of glass fiber reinforced plastics (GFRP C1, GFRP C2, GFRP C3, GFRP C4, GFRP C5, GFRP C6, GFRP C7) and carbon fiber reinforced plastics (CFRP C1, CFRP C2, CFRP C3, CFRP C4, CFRP C5, CFRP C6, CFRP C7).

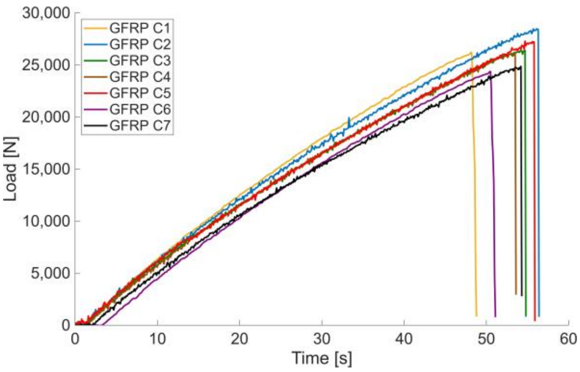

a)

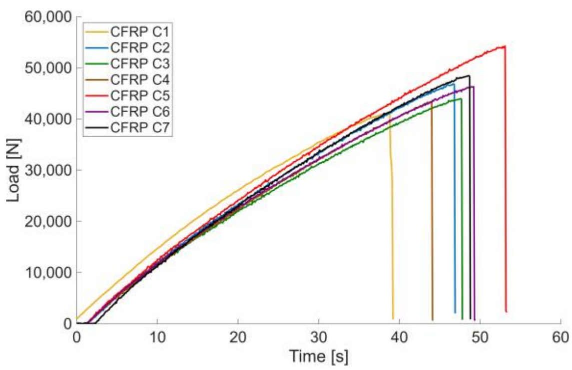

b)

Fig. 5. Force-time curves during compression testing of GFRP (a) and CFRP (b)

The plots presented allow for the determination of the average maximum compressive force occurring prior to specimen failure. The average maximum compressive force for GFRP was 26,769.61 N, and for CFRP it was 47,141.43 N. The cross-sectional areas of the compressed specimens were 82.54 mm² (GFRP) and 81.15 mm² (CFRP), corresponding to compressive strengths of 324.3 MPa for GFRP and 580.9 MPa for CFRP.

The fracture area of the specimen during the compression test of GFRP and CFRP is shown in Fig. 6. The color scale indicates the percentage of displacement in each of the tested composites.

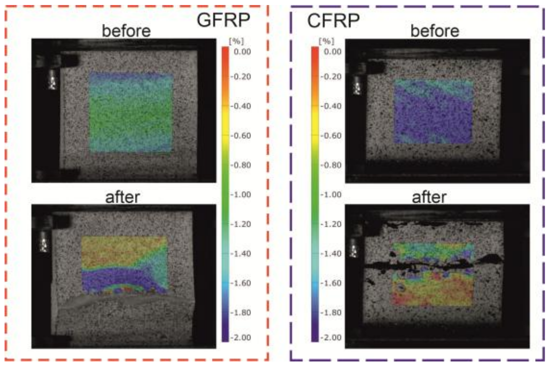

Fig. 6. Visualization of compression test specimens made of GFRP and CFRP

The final test involved conducting a shear test on composite specimens in accordance with ASTM D3518. The specimens were designated as GFRP S1, GFRP S2, GFRP S3, GFRP S4, GFRP S5, GFRP S6, and GFRP S7 for the glass fiber reinforced plastics, and as CFRP S1, CFRP S2, CFRP S3, CFRP S4, CFRP S5, CFRP S6, and CFRP S7 for the carbon fiber reinforced plastics. As in previous tests, seven specimens were prepared for the shear test. The force-time curves obtained during the shear tests for GFRP and CFRP specimens are presented in Fig. 7.

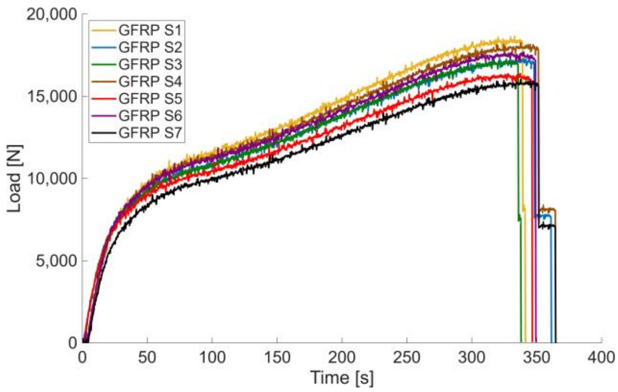

a)

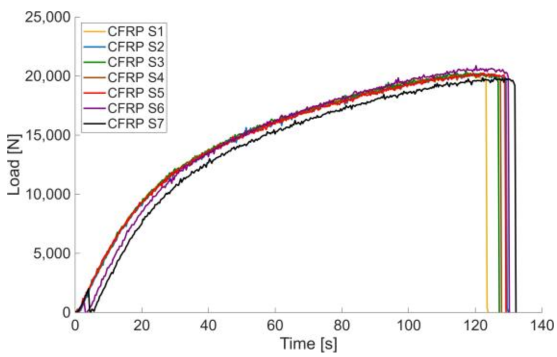

b)

Fig. 7. Force-time curves during shear testing of GFRP (a) and CFRP (b)

Based on the tests and plots, the average maximum shear force was 16,381.55 N for GFRP and 19,891.94 N for CFRP. The cross-sectional area of the specimen subjected to the shear test was 77.80 mm² (GFRP) and 77.02 mm² (CFRP). Based on Equation (8), the shear strength of GFRP is 105.3 MPa, and for CFRP it is 129.3 MPa.

The use of DIC in shear testing enabled capturing images of the material specimen before and after cracking. Fig. 8 shows the specimens before and after failure for both composite types.

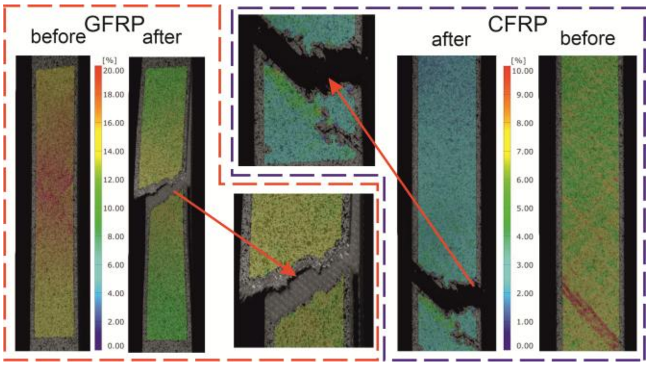

Fig. 8. Visualization of shear test specimens made of GFRP and CFRP

After conducting tensile, compression, and shear tests on a testing machine, the results were analyzed using Zeiss Inspect Correlate 2025 software, which utilized the Tensile Test Preparation and Tensile Test Evaluation scripts. The software, which incorporated relevant standards, was used to enter the cross-sectional dimensions of the specimens measured prior to the strength tests. As a result of the calculations performed in the software, it was possible to determine Young's modulus and Poisson's ratio in the tensile test, as well as shear modulus in the shear test for fabric-based composites. The structure of the fabric, composed of alternately arranged perpendicular fibers, indicates that the obtained values are identical in both loading directions. Tables 1–6 present all test values for polymer composites with glass and carbon fibers, along with the average values adopted for further analysis and the corresponding standard deviations.

Tab. 1. Values obtained from tensile tests on GFRP

Testing	Load F_t [N]	Strength σ_t [MPa]	Young's modulus E_{12} [MPa]	Poisson's ratio v_{12} [-]
Tensile	27548.64	448.70	21501.20	0.255
	27396.68	457.42	21518.82	0.246
	27172.71	430.80	20765.74	0.257
	25241.36	390.87	20520.75	0.259
	25481.20	401.45	20069.60	0.251
	26686.65	415.65	20175.40	0.238
	26453.99	430.80	21574.90	0.259
Average value	26568.75	425.10	20875.20	0.25
Standard deviation	911.25	24.11	654.73	0.01

Tab. 2. Values obtained from compression tests on GFRP

Testing	Load F_c [N]	Strength σ_c [MPa]
Compressive	27596.88	332.17
	28462.08	348.65
	27374.58	322.5
	27166.63	321.5
	27278.38	336.54
	24610.36	302.6
	24898.38	306.15
Average value	26769.61	324.30
Standard deviation	1443.10	16.41

Tab. 3. Values obtained from shear tests on GFRP

Testing	Load F_s [N]	Strength τ_s [MPa]	Shear modulus G_{12} [MPa]
Shear	17007.24	109.65	5418.17
	16183.05	103.94	5429.877
	17803.09	114.86	5543.213
	17057.65	108.656	5481.361
	15887.19	103.65	5449.149
	15486.12	98.78	5476.05
	15246.53	97.55	5452.98
Average value	16381.55	105.30	5464.40
Standard deviation	934.81	6.17	41.49

Tab. 4. Values obtained from tensile tests on CFRP

Testing	Load F_t [N]	Strength σ_t [MPa]	Young's modulus E_{12} [MPa]	Poisson's ratio v_{12} [-]
Tensile	37392.69	608.65	60630.40	0.310
	33887.93	551.77	60001.01	0.325
	38841.96	629.06	61171.65	0.297
	32827.38	522.52	59388.83	0.304
	35282.80	569.38	60419.08	0.324
	37345.21	572.64	60986.65	0.338
	37186.79	587.79	59657.76	0.308
Average value	36109.25	577.40	60322.20	0.32
Standard deviation	2167.62	35.38	668.74	0.01

Tab. 5. Values obtained from compression tests on CFRP

Testing	Load F_c [N]	Strength σ_c [MPa]
Compressive	48837.84	602.54
	47533.71	590.28
	43978.41	542.40
	44286.56	544.42
	54568.47	670.15
	42388.68	521.03
	48396.32	595.54
Average value	47141.43	580.90
Standard deviation	4092.82	50.23

Tab. 6. Values obtained from shear tests on CFRP

Testing	Load F_s [N]	Strength τ_s [MPa]	Shear modulus G_{12} [MPa]
Shear	20057.60	137.85	8066.56
	19298.39	129.32	7766.30
	19962.32	128.99	7535.78
	19846.36	128.14	7687.80
	19746.36	128.45	7943.95
	19986.21	130.75	7589.2
	20346.36	121.62	8011.12
Average value	19891.94	129.30	7800.10
Standard deviation	322.32	4.77	209.89

Table 7 presents a comprehensive summary of the average test results for the mechanical and strength properties of polymer composites based on glass and carbon fibers impregnated with epoxy resin, manufactured from prepregs in bidirectional fabric form.

Tab. 7. Material parameters of the polymer composites

Parameter	GFRP	CFRP
Density [g/cm^3]	1.698	1.513
Young's modulus E_{12} [MPa]	20875.2	60322.2
Shear modulus G_{12} [MPa]	5464.4	7800.1
Poisson's ratio ν_{12} [-]	0.25	0.32
Tensile strength σ_t [MPa]	425.1	577.4
Compressive stre-ngth σ_c [MPa]	324.3	580.9
Shear strength τ_s [MPa]	105.3	129.3

The mechanical and strength properties presented in Table 7 were compared with published data available for fabric GFRP and CFRP epoxy laminates. Direct quantitative comparison between different studies should be made with caution because the reported properties strongly depend on the fiber architecture, fiber volume fraction, resin system, curing cycle, laminate thickness, and testing methodology.

Nevertheless, the experimentally determined Young's modulus, tensile strength, compressive strength, and shear properties obtained in the present study fall within the ranges reported for comparable fabric epoxy laminates manufactured using prepreg technology. Similar observations have been reported for autoclave-manufactured CFRP laminates by [36] and [37], as well as for fabric carbon/epoxy laminates tested according to ASTM tensile and compression procedures [14]. In particular, the fabric CFRP laminates investigated in [36] exhibited a Young's modulus of approximately 34.45 GPa and a shear modulus of 2.87 GPa. Although these values are lower than those obtained in the present study, the differences can be attributed to variations in the fiber architecture, fiber volume fraction, resin system, and manufacturing conditions.

For GFRP laminates, comparable mechanical behavior has also been reported for fabric glass fiber/epoxy composites, although differences in fiber architecture, fiber volume fraction, and manufacturing technology influence the final mechanical properties. It should also be noted that the majority of published studies report the mechanical properties of unidirectional composite laminates rather than woven fabric laminates. For example, Young's modulus and Poisson's ratio reported for unidirectional GFRP are 50.40 GPa and 0.296, respectively, while corresponding values for unidirectional CFRP are 123.53 GPa and 0.351 [38]. These values are considerably higher than those obtained in the present work, which is expected because unidirectional laminates exhibit superior stiffness and load-carrying capability in the fiber direction compared with bidirectional fabric laminates. Consequently, the differences observed between the present results and the literature are consistent with the influence of reinforcement architecture on the mechanical response of polymer composite laminates.

The mechanical and strength parameters obtained for the composite materials will be used in numerical simulations (FEM). The results will enable accurate modeling of the behavior of polymer composites during machining.

4. CONCLUSIONS

This paper presents experimental studies aimed at determining the mechanical and strength properties of polymer composites made with glass fiber reinforced plastics (GFRP) and carbon fiber reinforced plastics (CFRP). The materials were fabricated from prepregs in the form of bidirectional epoxy-impregnated fabrics. For tensile testing, material specimens were prepared in accordance with ASTM D3039. Compression testing was performed on material specimens prepared in accordance with ASTM D6641, and shear testing was performed on specimens specified in ASTM D3518. The tests described in this paper allowed for the determination of mean values and their standard deviations. Based on the experimental results, the average Young's modulus of GFRP (20,875.20 MPa) was determined, which is approximately three times lower than Young's modulus for CFRP, which was 60,322.2 MPa. In the tensile test, the maximum tensile forces for GFRP (26,568.75 N) and CFRP (36,109.25 N) were also measured, allowing the tensile strengths of both materials to be determined: 425.1 MPa for GFRP and 577.4 MPa for CFRP. The compression test was used to determine the maximum compressive force and compressive strength for GFRP (26,769.61 N and 324.3 MPa) and CFRP (47,141.43 N and 580.9 MPa). In the final stage of the research, namely the shear tests of composite specimens, the maximum shear force (16,381.55 N for GFRP, 19,891.94 N for CFRP) and shear strength (105.3 MPa for GFRP, 129.3 MPa for CFRP) were determined. As part of this study, the shear modulus was also determined at 5,464.4 MPa for GFRP and 7,800.1 MPa for CFRP.

The obtained experimental database provides reliable input data for future numerical modeling of GFRP and CFRP structures. The use of identical manufacturing conditions, standardized ASTM testing procedures, and full-field DIC measurements enabled a consistent comparison between both composite systems and supports future validation of finite element models.

Further scientific work related to the machining of polymer composites will involve conducting numerical simulations based on the determined parameters. The simulations will also be validated through experimental research. The generated material dataset may also facilitate future research on machining, structural design, and failure analysis of polymer composite components.

REFERENCES

1. Fernández J, Pernía A, Martínez-de-Pisón FJ et al. Prediction models for calculating bolted connections using data mining techniques and the finite element method. Engineering Structures 2010;32(10):3018–27. https://doi.org/10.1016/j.engstruct.2010.05.021
2. Sahinoglu M. Modeling and simulation in engineering. WIREs Computational Stats 2013;5(3):239–66. https://doi.org/10.1002/wics.1254
3. Krzywanski J, Sosnowski M, Grabowska K et al. Advanced Computational Methods for Modeling, Prediction and Optimization-A Review. Materials 2024;17(14):3521. https://doi.org/10.3390/ma17143521
4. Pal B, Riyazuddin Haseebuddin M. Analytical Estimation of Elastic Properties of Polypropylene Fiber Matrix Composite by Finite Element Analysis. AMPC 2012;02(01):23–30. https://doi.org/10.4236/ampc.2012.21004
5. Ji X, Xu Y, Zhang W et al. Review of functionalization, structure and properties of graphene/polymer composite fibers. Composites Part A: Applied Science and Manufacturing 2016;87:29–45. https://doi.org/10.1016/j.compositesa.2016.04.011
6. Bukvić M, Milojević S, Gajević S et al. Production Technologies and Application of Polymer Composites in Engineering: A Review. Polymers 2025;17(16):2187. https://doi.org/10.3390/polym17162187
7. Zike S, Mikkelsen LP. Correction of Gauge Factor for Strain Gauges Used in Polymer Composite Testing. Exp Mech 2014;54(3):393–403. https://doi.org/10.1007/s11340-013-9813-7.
8. Różyło P, Smagowski W, Paśnik J. Experimental Research in the Aspect of Determining the Mechanical and Strength Properties of the Composite Material Made of Carbon-Epoxy Composite. Adv Sci Technol Res J 2023;17(2):232–46. https://doi.org/10.12913/22998624/161598
9. Penner E, Caylak I, Mahnken R. Experimental Investigations of Carbon Fiber Reinforced Polymer Composites and Their Constituents to Determine Their Elastic Material Properties and Complementary Inhomogeneous Experiments with Local Strain Considerations. Fibers Polym. 2023. https://doi.org/10.1007/s12221-023-00122-x
10. Georgousis G, Pandis C, Kalamiotis A et al. Strain sensing in polymer/carbon nanotube composites by electrical resistance measurement. Composites Part B: Engineering 2015;68:162–69. https://doi.org/10.1016/j.compositesb.2014.08.027
11. Sanchez-Sobrado O, Rodriguez D, Losada R et al. Evaluation of conductive smart composite polymeric materials for potential applicationsin structural health monitoring and strain detection. Functional Composite Mater 2023;4(1):2. https://doi.org/10.1186/s42252-023-00039-x
12. Mehar A, Ahmed GMS, Kumar GP et al. Experimental Investigation and FE Analysis of CFRP Composites. Materials Today: Proceedings 2015;2(4–5):2831–2839. https://doi.org/10.1016/j.matpr.2015.07.297
13. Munoz V, Perrin M, Pastor ML et al. Determination of the elastic properties in CFRP composites: comparison of different approaches based on tensile tests and ultrasonic characterization. Advances in Aircraft and Spacecraft Science 2015;2(3):249–61. https://doi.org/10.12989/AAS.2015.2.3.249
14. Liu F, Grotz L, Cui Y et al. Experimental dataset on the in-plane tensile, shear, and compressive properties of a carbon-epoxy twill woven composite. Data in Brief 2022;45:108650. https://doi.org/10.1016/j.dib.2022.108650
15. Laurin F, Charrier JS, Lévêque D et al. Determination of the Properties of Composite Materials Thanks to Digital Image Correlation Measurements. Procedia IUTAM 2012;4:106–15. https://doi.org/10.1016/j.piutam.2012.05.012
16. Golewski P, Sadowski T, Kneć M et al. The effect of thermal aging degradation of CFRP composite on its mechanical properties using destructive and non-destructive methods and the DIC system. Polymer Testing 2023;118:107902. https://doi.org/10.1016/j.polymertesting.2022.107902
17. Rahmatabadi D, Shahmirzaloo A, Farahani M et al. Characterizing the elastic and plastic properties of the multilayered Al/Brass composite produced by ARB using DIC. Materials Science and Engineering: A 2019;753:70–8. https://doi.org/10.1016/j.msea.2019.03.002
18. Sadowski T, Knec M. Application of Dic Technique for Monitoring of Deformation Process of Spr Hybrid Joints/Zastosowanie Techniki Dic Do Obserwacji Procesu Deformacji Hybrydowych Połaczen Typu Spr. Archives of Metallurgy and Materials 2013;58(1):119–25. https://doi.org/10.2478/v10172-012-0161-x
19. Del Rey Castillo E, Allen T, Henry R et al. Digital image correlation (DIC) for measurement of strains and displacements in coarse, low volume-fraction FRP composites used in civil infrastructure. Composite Structures 2019;212:43–57. https://doi.org/10.1016/j.compstruct.2019.01.024
20. Hong C, Park M, Ji W. Synchronous application of DIC and DVC techniques for the global-local characterization of carbon fiber-reinforced composite laminates. Polymer Testing 2025;145:108757. https://doi.org/10.1016/j.polymertesting.2025.108757
21. Jelić A, Sekulić M, Travica M et al. Determination of Mechanical Properties of Epoxy Composite Materials Reinforced with Silicate Nanofillers Using Digital Image Correlation (DIC). Polymers 2022;14(6):1255. https://doi.org/10.3390/polym14061255
22. Wang B, Zhong S, Lee TL et al. Non-destructive testing and evaluation of composite materials/structures: A state-of-the-art review. Advances in Mechanical Engineering 2020;12(4):168781402091376. https://doi.org/10.1177/1687814020913761
23. Xu D, Cerbu C, Wang H et al. Analysis of the hybrid composite materials reinforced with natural fibers considering digital image correlation (DIC) measurements. Mechanics of Materials 2019;135:46–56. https://doi.org/10.1016/j.mechmat.2019.05.001
24. Ziaja D, Jurek M, Śliwa R et al. DIC application for damage detection in FRP composite specimens based on an example of a shearing test. Arch Civ Mech Eng 2024;24(1):47. https://doi.org/10.1007/s43452-024-00859-z
25. Tekieli M, De Santis S, De Felice G et al. Application of Digital Image Correlation to composite reinforcements testing. Composite Structures 2017;160:670–688. https://doi.org/10.1016/j.compstruct.2016.10.096
26. Feng W, He P, Pavlovic M. Combined DIC and FEA method for analysing debonding crack propagation in fatigue experiments on wrapped composite joints. Composite Structures 2022;297:115977. https://doi.org/10.1016/j.compstruct.2022.115977
27. Venkatachalam S, Khaja Mohiddin SM, Murthy H. Determination of damage evolution in CFRP subjected to cyclic loading using DIC. Fatigue Fract Eng Mat Struct 2018;41(6):1412–1425. https://doi.org/10.1111/ffe.12786
28. Montesano J, Selezneva M, Levesque M et al. Modeling fatigue damage evolution in polymer matrix composite structures and validation using in-situ digital image correlation. Composite Structures 2015;125:354–61. https://doi.org/10.1016/j.compstruct.2015.02.035
29. Calvo JV, Feito N, Miguélez MH et al. Modeling the delamination failure under compressive loads in CFRP laminates based on digital image correlation analysis. Composite Structures 2022;287:115265. https://doi.org/10.1016/j.compstruct.2022.115265
30. Wang Y, Luo Q, Xie H et al. Digital image correlation (DIC) based damage detection for CFRP laminates by using machine learning based image semantic segmentation. International Journal of Mechanical Sciences 2022;230:107529. https://doi.org/10.1016/j.ijmecsci.2022.107529
31. Rizo-Patron S, Sirohi J. Operational Modal Analysis of a Helicopter Rotor Blade Using Digital Image Correlation. Exp Mech 2017;57(3):367–75. https://doi.org/10.1007/s11340-016-0230-6
32. LeBlanc B, Niezrecki C, Avitabile P. Structural health monitoring of helicopter hard landing using 3D digital image correlation, ed. Kundu T. San Diego, California, USA, 2010, 76501V. https://doi.org/10.1117/12.847318
33. ASTM D3039/D3039M-17, Standard Test Method for Tensile Properties of Polymer Matrix Composite Materials. ASTM International, West Conshohocken, PA, 2017. n.d.
34. ASTM D6641/D6641M-23, Standard Test Method for Compressive Properties of Polymer Matrix Composite Materials Using a Combined

Loading Compression (CLC) Test Fixture, ASTM International, West Conshohocken, PA, 2016. n.d.
35. ASTM D3518/D3518M-18, Standard Test Method for In-Plane Shear Response of Polymer Matrix Composite Materials by Tensile Test of a +/- 45° Laminate. ASTM International, West Conshohocken, PA, 2018. n.d.
36. Wiggers H, Ferro O, Sales RDCM et al. Comparison between the mechanical properties of carbon/epoxy laminates manufactured by autoclave and pressurized prepreg. Polymer Composites 2018;39(S4). https://doi.org/10.1002/pc.24842
37. Bergant Z, Savin A, Grum J. Effects of manufacturing technology on static, multi-frequency dynamic mechanical analysis and fracture energy of cross-ply and quasi-isotropic carbon/epoxy laminates. Polymers and Polymer Composites 2018;26(5–6):358–70. https://doi.org/10.1177/0967391118798266
38. Gfrerrer M, Pires VDC, Brunner AJ et al. Comparing the In-Plane Shear Behavior of Glass Fiber-Reinforced and Carbon Fiber-Reinforced Polymer Laminates With the Same Epoxy Matrix System in ±45° Tensile Tests. Polymer Composites 2026;47(12):11051–68. https://doi.org/10.1002/pc.71004

Krzysztof Ciecieląg: https://orcid.org/0000-0003-1336-0438